Desalination and Water Treatment
www.deswater.com

doi:10.5004/dwt.2019.23124

139 (2019) 133–144
January

Study of the application of a self-made ultrafine grinding catalytic internal electrolytic filler in pulping wastewater pretreatment

Luting Pan[a,*], Guijiao Lin[a], Jiucheng Wang[a,b], Ajun Wan[a,*], Xinjue Xie[a], Yixuan Xie[a], Runqiu Tu[a]

[a]*Institute of New Rural Development, Tongji University, Shanghai 201804, China, email: lutingpan@163.com (L. Pan), lgj1310476223@163.com (G. Lin), 394138641@qq.com (J. Wang), wanajun@tongji.edu.cn (A. Wan), yixuanxie95@163.com (Y. Xie), 597726526@qq.com (R. Tu)*
[b]*Tus-Design Group Co., Ltd, Jiangsu Suzhou 21500, China*

Received 18 January 2018; Accepted 12 September 2018

ABSTRACT

A pilot scale experiment was conducted to investigate the characteristics and factors that influence contaminant removal in a pulping wastewater pretreatment process, which was treated by a self-made ultrafine grinding catalytic internal electrolytic filler. The powder metallurgy method was used to prepare the novel filler, with iron powder, graphite powder, copper powder and manganese powder as the raw materials. A comparative study conducted with commercial packing material under the same conditions showed that the self-made filler performed better than the commercial material regarding pollutant removal. COD_{Cr} and the chroma removal rate were used as evaluation indexes, and a single factor test and L27 (3^{13}) orthogonal test were utilized to obtain the optimum working conditions and interaction effects of each influencing factor. At the same time, using SEM to observe the surface morphology and structural change of the filler and analyzing the IR spectra of wastewater and sediment before and after the reaction, the reaction mechanism and organic degradation mechanism were discussed.

Keywords: Pulping wastewater; Internal electrolytic packing; Optimum condition; COD and chroma removal rate

1. Introduction

Pulping wastewater is known to be one of the most refractory industrial sewages because of its complex composition, refractory substances contents, high chroma, and limited biodegradation, so it generally requires little pretreatment. Currently, the pretreatment approaches are coagulation precipitation, oxidation, and the electrochemical method [1–3]. The coagulation treatment process causes secondary pollution and requires maintenance costs [4]. The oxidation-reduction process has the disadvantage of selective oxidation and incomplete processing [5]. For the electrochemical method, the requirement of a large amount of energy and electrode materials results in large quantities of sewage [6].

To address these problems, the catalytic internal electrolysis method was introduced in this study. The principle of the catalytic internal electrolysis method is that wastewater serves as an electrolyte solution in which numerous iron-carbon primary cell reactions occur due to the addition of inert substances (such as activated carbon and graphite) and some high-potential metals to cast-iron scrap [7]. The mechanisms involved in this method can be summarized as follows: electro chemistry, oxidization and reduction, electric enrichment, flocculation, precipitation and adsorption. Compared with other methods, this process has the ability to improve biodegradability, maintain a stable effect and accelerate organic compound degradation [8]. Hence, the catalytic internal electrolysis method is widely used for the

*Corresponding author.

pretreatment of difficult biodegradable organic wastewater from sources such as the paper making industry, printing and dyeing industry, pharmaceutical industry, coking plants, petrochemical industry and so on [9–11]. Although internal electrolysis performs well in treating wastewater, it is frequently found that the normal filler used in practical projects has a short service life and low processing efficiency due to compaction and passivation of fillers.

Therefore, to overcome the problems associated with using normal fillers, we used the powder metallurgy method to generate an ultrafine grinding catalytic internal electrolytic filler. During this process, we raised the unit number of corrosive microcells by reducing the packing size and improving the uniformity of the distribution. Finally, we acquired a self-made ultrafine grinding catalytic internal electrolytic filler that had an excellent performance. Compaction and passivation of the filler were significantly alleviated, the service life expectancy increased, and the treatment effect became more stable. Additionally, comparative experiments were conducted to study the unique advantages of this filler, and at the same time, to further analyze the effects of organic compounds in the system effluent and precipitants on the filler surface, experiments were conducted to investigate the characteristics and mechanisms of pollutant removal from the system. In this paper, a method of preparing a new and efficient internal electrolytic packing was is described, which expands the filler preparation methods and performance studies.

2. Materials and methods

2.1. Experimental water

The raw wastewater used in this study was from a paper mill in a rural area (Jiangsu province, China). The parameters of the wastewater samples are shown in Table 1. All samples were stored at 4°C and analyzed within 24 h.

2.2. Apparatus and experimental procedures

The experimental apparatus used is shown in Fig. 1; a moderate amount of wastewater was used in the reactor, and variables such as the pH level and aeration quantity were adjusted to set values. After a certain period of time, PAM were added for coagulation and precipitation. The wastewater was filtered through a 0.45 μm Millipore filter, and its COD_{Cr} concentration and chroma were determined.

Table 1
Characteristics of raw wastewater

COD, mg·L^{-1}	3000–3200
BOD_5, mg·L^{-1}	850–1000
NH_3-N, mg·L^{-1}	60–100
TN, mg·L^{-1}	120–150
TP, mg·L^{-1}	3–5
SS, mg·L^{-1}	200–350
pH	5.5–7.5

2.3. Test methods

All samples were stored at 4°C and analyzed within 24 h. According to the standard methods (Environmental Protection Agency (EPA) of China, 1989), the chemical oxygen demand $(COD)_{Cr}$ concentrations of the samples were determined using the potassium dichromate method. The pH value was determined using a pH meter (Model 252, Thermo Orion). The colorimetric test was performed using the Canadian Pulp and Paper Association (CPPA) standard method. The specific method is to adjust the pH of the water sample to 7.6 ± 0.1 with 1.0 mol/L of a NaOH and H_2SO_4 solution, filter the water sample through a 0.45 μm nylon filter membrane, and measure the absorbance of the filtered sample at a maximum absorption wavelength of 465 nm. According to Eq. (1), the absorbance value was converted to a standard color value C.U. (Color Unit) [12,13]. If the water sample required dilution, dilute it with diluted with a phosphate and phosphate buffer solution (pH value 7.6 ± 0.1).

$$\text{Colorimetric}(\text{C.U.}) = 500\frac{\text{A2}}{\text{A1}}\text{D} \quad (1)$$

In the equation, A1: Absorbance of a 500 C.U. platinum cobalt solution at 465 nm, 0.132; A2: Absorbance of the water sample at 465 nm; D: Dilution multiple of the water sample.

2.4. Analytical methods

First, the optimal values of reaction time, initial pH value, aeration volume and filler dosage for the COD and color removal were determined by a single factor test method. Then, an orthogonal experimental design was applied to observe the significant differences and correlations between these four factors. Finally, Minitab15 software was used to perform variance analysis, Taguchi analysis and interaction analysis of the experimental data to identify the factors that had the greatest influence on the performance of the catalytic internal electrolysis and to determine the optimum experimental conditions.

3. Results and discussion

3.1. Effect of the reaction time

To what extent the chemical reaction proceeds and whether the reaction is complete or not is determined by the length of the reaction time [14]. An insufficient reaction time will lead to an incomplete reaction, and a longer reaction time will increase the consumption of the filler and require a larger volume for the reaction. In the experiment, the effects of the reaction time on the COD and chromaticity removal were studied when the reaction time was 0.5 h, 1 h, 1.5 h, 2 h and 2.5 h, with an initial pH of 3.0, aeration quantity of 1 L/min, and amount of fillers of 1 g/mL.

The results regarding the variance of the removal rate of the COD and chroma with the reaction time are presented in Fig. 2. As shown in Fig. 2a, when the reaction time was 0.5 h, 1.5 h, and 2.5 h, the corresponding COD removal rates were 31%, 39%, and 41%, respectively, peaking at 2.5 h. The results indicate that the appropriate length of the reaction time is beneficial to organic compound degradation

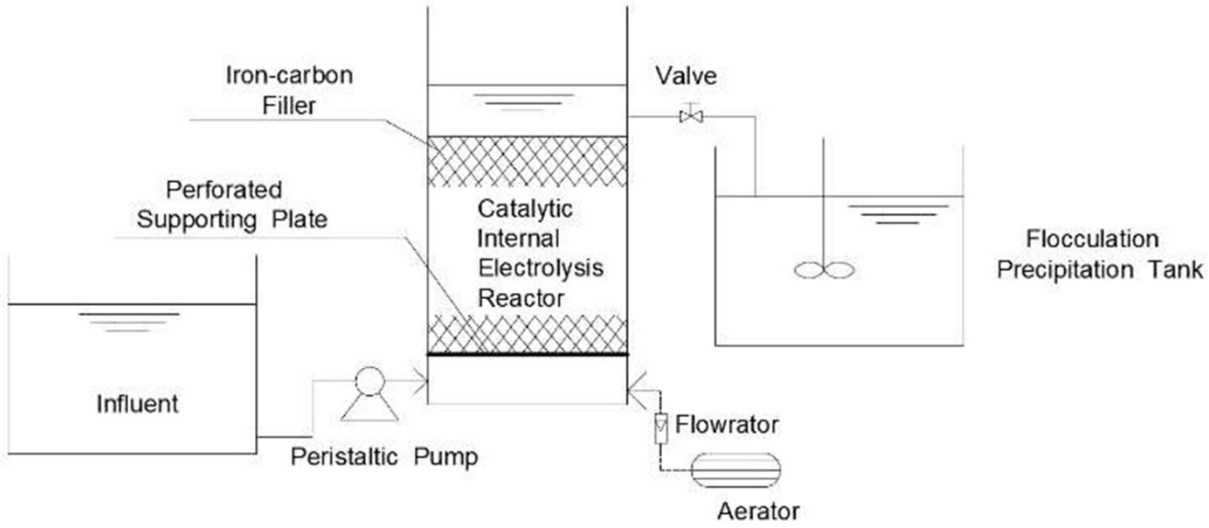

Fig. 1. Devices for pulping wastewater treatment by catalyzed internal electrolysis.

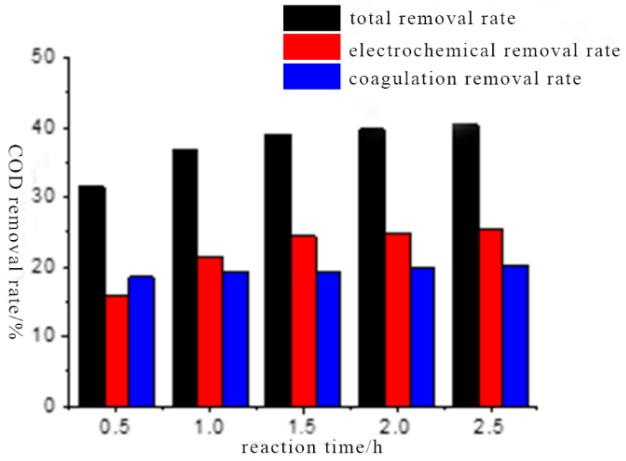

(a)

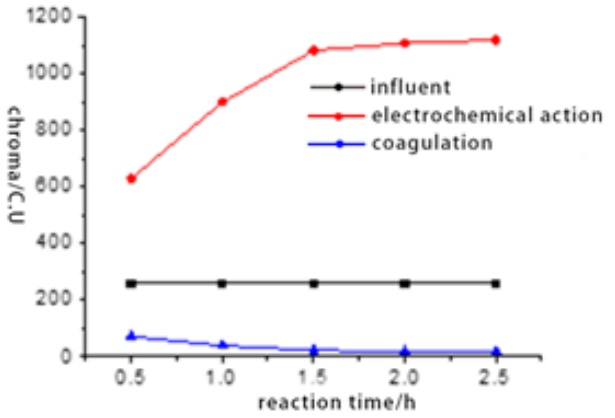

(b)

Fig. 2 Effect of the reaction time on the COD and chroma: (a) COD; (b) chroma.

and chroma reduction. In addition, with the extension of the reaction time, various synergistic effects of the internal electrolysis were more complete. However, when the reaction time exceeded 1.5 h, as the reaction consumed H^+, the potential difference of the electrode was reduced, corrosion of the micro-battery was weakened, and internal electrolysis efficiency was decreased according to the electrode reaction equation. Hence, the COD removal rate increases slowly in longer reactions.

As revealed by Fig. 2b, the removal rate of the chroma increased more quickly with reaction times from 0.5 h–1.0 h than reaction times from 1 h to 1.5 h. When the reaction time was longer than 1.5 h, the chroma removal rate remained static and peaked at 2.5 h because the extension of the reaction time increases iron corrosion, which generates more Fe^{2+} in solution; under aeration, Fe^{2+} is oxidized to Fe^{3+}, resulting in an increase in chromaticity. After the coagulation reaction, the color of the solution first decreased and then became stable because Fe^{2+} and Fe^{3+} react with OH– to form $Fe(OH)_2$ and $Fe(OH)_3$, respectively, and then, strong hydrolysis reaction takes place, resulting in a longer linear structure of the hydroxyl complexes, such as $Fe(OH)^{2+}$, $Fe(OH)^{2+}$, and so on. These hydroxyl complexes have a porous gel structure and strong adsorption, which can play the role of flocculation adsorption, so the wastewater has a slight decolorization effect.

Therefore, by taking the effect of each index into account, the optimal reaction time was found to be 1.5 h, leading to COD and chroma removal rates of 39.1% and 91.1%, respectively.

3.2. *Effect of the initial pH value*

The initial pH value can affect the performance of the internal electrolysis filler and control the corrosion rate of iron. The initial pH value serves a double purpose of destroying pollutants and maintaining the acid-base balance of the whole system since internal electrolysis is capable of producing OH^- or consuming extra H^+ in a system

with a different pH [15]. Meanwhile, in neutral and alkalescent environments, Fe^{2+} and Fe^{3+} derived from the internal electrolysis reaction exert positive effects on pollutant removal owing to their strong flocculating activity. The impact of the pH value on COD and chroma removal was observed when the reaction time was set at 1.5 h, aeration quantity at 1 L/min, and dosage of the filler added at 1 g/mL. The results are presented in Fig. 3.

Fig. 3a suggests that the total COD removal efficiency of the whole system experienced an upward and then downward trend as the pH value decreased. The total COD removal efficiency reached a relatively high level under the slightly acidic condition, where the corrosion that occurred on the filler surface was accelerated, leading to the degradation of organics through electrochemical action. Thus, total COD removal peaked at 37.7% when the pH value was 3 because, according to the Nernst equation, the lower the pH level, the higher the electrode potential of the cathode, which leads to greater potential differences between the electrodes of the iron-carbon primary cell. Large potential differences can accelerate the electrode reaction and improve the treatment performance by accelerating iron corrosion and allowing oxidation reduction, electricflocculation and adsorption.

It is observed from Fig. 3b that the wastewater chroma removal rate first increased and then decreased with the increase of the pH. When the initial pH was 1.0, 3.0, and 7.0, the corresponding chromaticity removal rate was 77.0%, 88.3%, and 81.2%, respectively, peaking at 3.0. When the initial pH was 3, the internal electrolysis solution was much more colored than at the other pH values and chroma was lower than at the other pH values after coagulation. Because the reaction rate of the corrosion of the internal electrolytic filler was the fastest under this condition, the anode dissolved a large number of iron ions, which contributed to compound degradation. In the subsequent coagulation and sedimentation stage, the floc formed was larger than at the other pH values and the total color removal rate was the highest.

However, these results do not mean that a lower pH is better. In a strong acid, a large amount of generated iron ion complexes would adhere to the filler surface, impede the reaction, and increase chromaticity. Thus, considering all of the results, an initial pH of 3 is regarded as optimum.

3.3. Effect of the aeration quantity

Aeration during catalytic internal electrolysis can play the role of stirring, allowing the filler and wastewater to fully contact dissolved oxygen. The bubbles resulting from aeration will assist in stirring the filler and increase friction, which is helpful for removing the passive film on the filler surface and accelerating the mass transfer rate of the reaction system [16]. To observe the effects of the aeration quantity on the COD and chroma removal rates, the initial aeration rates used were 1.0 L/min, 0.5 L/min, 1.0 L/min, 1.5 L/min and 2.0 L/min under the initial conditions of a pH of 3.0, reaction time of 1.5 h, and filler dosage of 1 g/mL. The results are shown in Fig. 4.

With reference to Fig. 4(a), we observe that the COD removal rate increased gradually as the aeration quantity increased and the COD removal rate was almost unchanged when the aeration quantity rose from 0 L/min to 2.0 L/min. These results suggested that a relatively excellent performance of COD removal was achieved when the aeration quantity was approximately 1.0 L/min. In excess of a certain range, the aeration quantity would have little effect on the removal of organics because most recalcitrant organics are reduced and cracked into intermediate products and oxygen is essential for the complete oxidation decomposition of those intermediates. An enhanced removal capacity of organics can be achieved via the aeration quantity. An appropriate increase of aeration can improve the treatment effect of wastewater.

As shown in Fig. 4b, with the increase of the aeration rate, the wastewater chroma removal rate continued to rise. However, the wastewater chroma removal rate rose slowly when the aeration quantity rose from 1.0 L/min to 2.0 L/min. The removal rate increased by 35% when the aeration quantity increased from 0 L/min to 1.0 L/min, while it increased by 4% when the aeration quantity increased from 1.0 L/min to

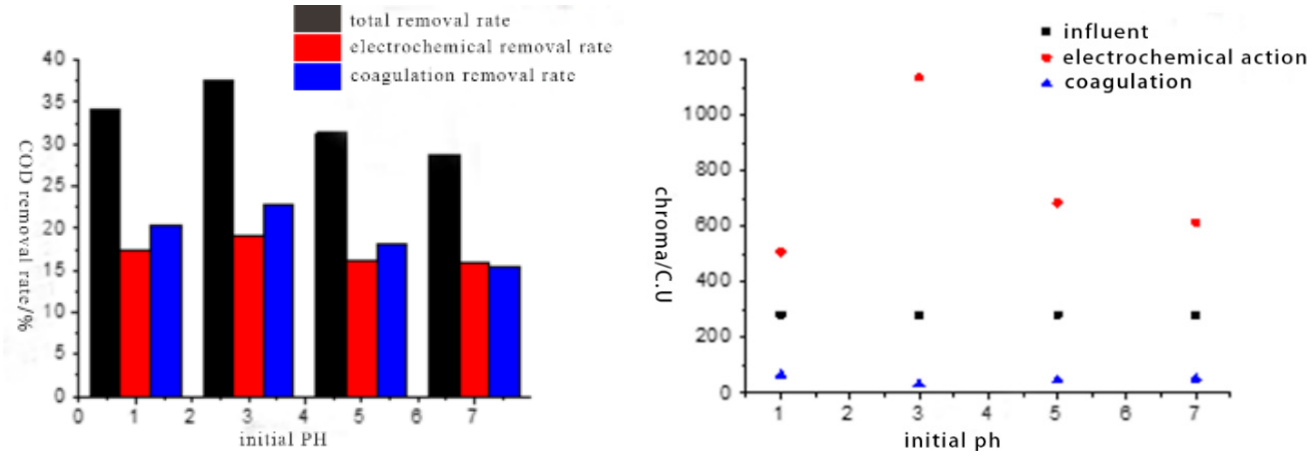

(a) (b)

Fig. 3. Effect of the initial pH value on the COD and chroma removal rates; (a) COD; (b) chroma.

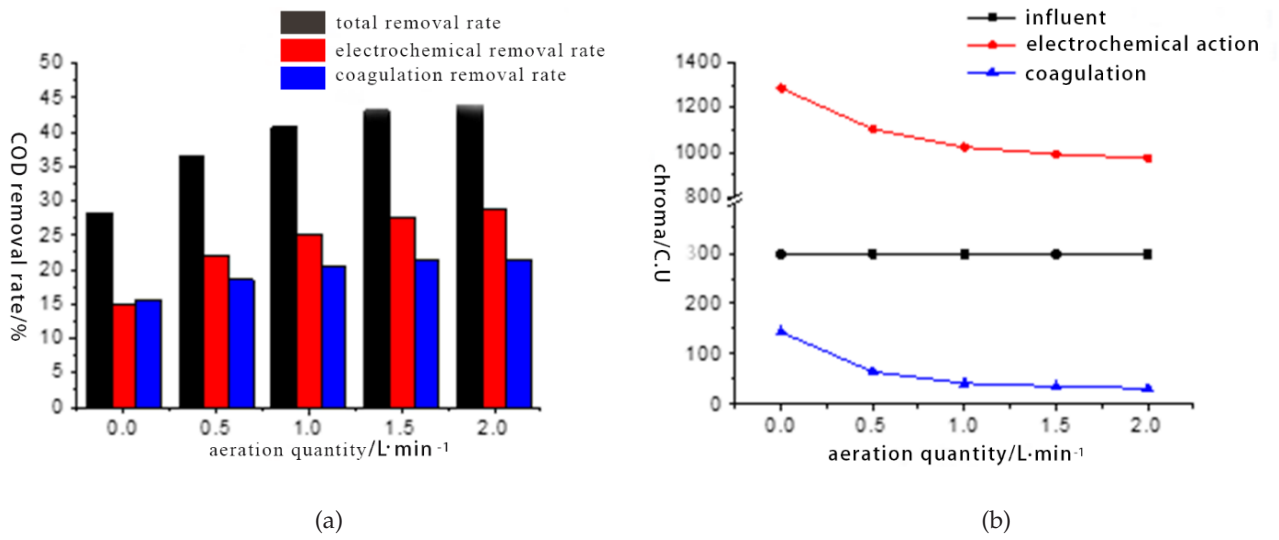

(a) (b)

Fig. 4. Effect of the aeration quantity on the COD and chroma removal rates: (a) COD; (b) chroma.

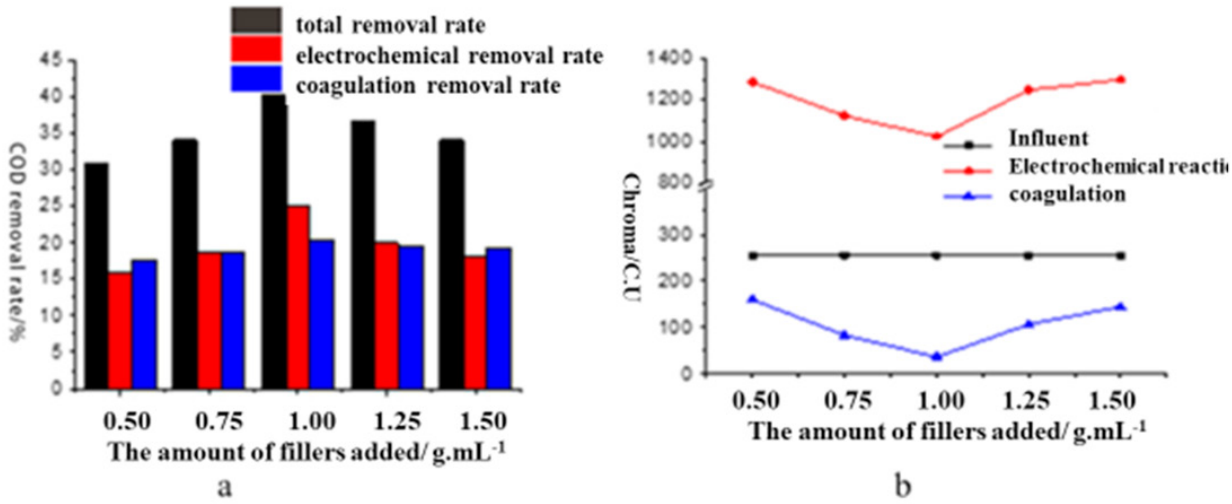

Fig. 5. Effect of the amount of fillers added on the COD and chroma removal rates: (a) COD; (b) chroma.

2.0 L/min. The reason for the smaller increase of the removal rate at a higher aeration quantity is that if the aeration volume is too large, the iron ion dissolution is too large, which increases the amount of chroma in solution. However, high aeration will increase the processing cost as well.

In summary, an aeration volume of 1.0 L/min is regarded as optimum, leading to COD and chroma removal rates of 40.7% and 85.9%, respectively.

3.4. Effect of amount of filler added

The effects of the different amounts of filler added on the removal of COD and chromaticity were investigated by experiments that were carried out with four amounts of filler, as follows: 0.5 g/mL, 0.75 g/mL, 1.0 g/mL, 1.25 g/mL and 1.5 g/mL, while the initial pH was 3.0, reaction time was 1.5 h, and aeration quantity was 1.0 L/min.

Table 2
Factor level of internal electrolysis orthogonal test

Factors	Levels		
	1	2	3
Reaction time (h)	1	1.5	2
Initial PH value	1	3	5
Aeration rate (L/min)	0.5	1	1.5
The amount of fillers added (g/mL)	0.5	1	1.5

As shown in Fig. 5, the total COD removal efficiency and color removal efficiency for the whole system increased first and decreased as the amount added fillers rose. When the substrate concentration was 1.0 g/mL, the removal efficiencies of COD and chroma peaked at 40.3% and 85.5%, respec-

tively. Meanwhile, the figure showing the electrochemistry stage showed a similar pattern to that of the whole system, whereas the coagulation stage was slightly influenced. It is observed from the above results that the removal of organic pollutants and chroma largely depended on the number of corroded cells; that is, better degradation of organics was achieved due to the increasing amount of fillers, which resulted in accelerated corrosion on the filler surface and thorough internal electrolysis. Nevertheless, the amount of added fillers increased the amount of dissolved Fe^{2+}. However, beyond a certain range, the effect of Fe^{2+} on the removal of the organics was not significant. Additionally, too much filler will increase the cost. Thus, addition of 1.0 g/mL filler the system was regarded as optimal.

4. Orthogonal experimental design

From the above analyses, it is suggested that four factors had significant impacts on COD and chroma removal and that there was a significant interaction ($P < 0.05$). The impact that the four factors had on COD removal was: amount of added fillers > reaction time > initial pH > aeration quantity. The impact that the four factors had on chroma removal was: amount of added fillers > aeration quantity > initial pH > reaction time (the larger F was, the greater its impacts were). After analyzing the significant differences, A3, B2, D2 and G2 (in Taguchi analysis, the greater the mean response, the higher the removal rates of COD and chromaticity) were the optimum conditions, that is, an initial pH level of 3.0, reaction time of 1.5 h, aeration quantity of 1.0 L/min and amount of added fillers of 1 g/mL.

5. Contrast experiment

To compare the effect of the self-made internal electrolytic filler and an ordinary filler on COD and color removal from pulping wastewater, a comparative experiment was designed using three types of internal electrolysis fillers: the self-made ultrafine grinding catalytic internal electrolytic filler (marked as 1# packing), a spherical internal electrolytic filler purchased from Wei Hua Dike Beijing Science and Technology Co. Ltd. (marked as 2# packing), and an oblate internal electrolytic filler purchased from Weifang XinHongyuan Environmental Protection Technology Co. Ltd (marked as 3# packing). Except for the different fillers, the other experimental conditions of the comparison experiments were exactly the same and were all operated under the optimum working conditions. The results are shown in Table 4.

The results provided in Table 4 illustrate that under the same working conditions, both the COD and chroma removal rates were higher in the experimental group using the self-made ultrafine grinding catalytic internal electrolytic filler compared to the normal packing fillers. In terms of COD removal, 1# had a superior removal capacity. Compared with 1#, the removal rate of 3# decreased by 10%. In terms of chroma removal, the experimental results showed that the chroma of the influent was 8 times greater than that of the effluent, while in the contrast group, the chroma of the influent was only 4 times greater than that of the effluent. It is obvious that the self-made filler has a superior capacity for chroma removal.

In this paper, a powder metallurgy method was used to obtain ultrafine powder catalyzed internal electrolytic fillers, the operational performance of which had been modified using smaller particle sizes, an even distribution of iron and carbon, and balanced consumption of micro-battery poles during corrosion by means of reducing the size of the powder particles as well as improving the distribution uniformity. In this way, based on improving the number of corrosive micro-batteries per filler surface area, hardening and passivation of the fillers were mitigated. Therefore, compared with the ordinary fillers, the treatment effect with the self-made internal electrolytic filler was better.

6. Reaction mechanism

6.1. SEM analysis

To determine the mechanism underlying COD and chroma removal by the catalytic internal electrolysis, a scanning electronmicroscope (SEM) was used to observe the surface morphology and structure of the internal electrolysis filler. Fig. 8 shows the results.

As observed from the SEM images, the filler surface before the reaction was smooth and had many holes. Previous research has shown that the reactions that occur on the iron-carbon surface mainly take place at bumps, pits, cracks and other defect sites, which are called reaction sites [17]. The filler surface after the reactions is rough, dissolved and covered with a large amount of precipitate adsorbed on the holes, which indicate that a galvanic reaction occurred on the surface of the filler, iron was consumed, and macromolecules were decomposed into small molecules adhering to the surface of the filler. The morphologic changes reduced the opportunity of wastewater to contact the packing, impeded mass transfer between them, and caused a lower reaction rate.

6.2 Infrared spectroscopy analysis

To further analyze the products generated during the reaction and to understand the mechanism underling COD and chroma removal by iron-carbon internal electrolysis, infrared spectroscopy was used to analyze the sediment on the surface of the filler, influent and effluent. The results are presented in Fig. 9.

The group of absorption peaks in the infrared spectrum of the influent and effluent shown in Fig. 9a are further described in Table 5 [18]. According to Table 5, the absorption peaks of 3420 cm^{-1} were due to OH telescopic vibrations of hydrogen bonding, and those at 2870 cm^{-1}, 2960 cm^{-1} were generated by the CH_3 bending vibration. The absorption peaks were only found i the effluent due to the f macromolecular materials in pulping wastewater being decomposed into small molecule intermediate products, such as CH_3. The absorption peaks in the range of 1620 cm^{-1}–1000 cm^{-1} mainly reflected carbonyl, benzene and ether bonds in the lignin structure; some of these peaks did not appear in the effluent spectrum, or some peaks were weaker and broader compared with those of the influent. From the above data, it is observed that the catalytic internal electrolysis reaction

Table 3
The design and results of orthogonal experiment for internal electrolysis

No	A	B	C	D	E	F	G	H	I	J	K	L	M	Removal rate of COD/%	Chromaticity removal rate/%
1	1(1)	1(1)	1(1×1)	1(0.5)	1(1×0.5)	1(1×0.5)	1(0.5)	1(1×0.5)	1	1(1×0.5)	1(0.5×0.5)	1	1	19.2	29.1
2	1(1)	1(1)	1(1×1)	1(0.5)	2(1×0.5)	2(1×0.5)	2(1)	2(1×1)	2	2(1×1)	2(0.5×1)	2	2	25.1	66.9
3	1(1)	1(1)	1(1×1)	1(0.5)	3(1×0.5)	3(1×0.5)	3(1.5)	3(1×1.5)	3	3(1×1.5)	3(0.5×1)	3	3	21.2	33.7
4	1(1)	2(2)	2(1×3)	2(1)	1(1×1)	1(3×1)	1(0.5)	2(1×0.5)	2	2(3×0.5)	3(1×0.5)	3	3	23.3	36.7
5	1(1)	2(2)	2(1×3)	2(1)	2(1×1)	2(3×1)	2(1)	3(1×1)	3	3(3×1)	1(1×1)	1	1	30.4	84.5
6	1(1)	2(2)	2(1×3)	2(1)	3(1×1)	3(3×1)	3(1.5)	1(1×1.5)	1	1(3×1.5)	2(1×1.5)	2	2	25.7	42.5
7	1(1)	3(5)	3(1×5)	3(1.5)	1(1×1.5)	1(5×1.5)	1(0.5)	3(1×0.5)	3	3(5×0.5)	2(1.5×0.5)	2	2	20.6	35.6
8	1(1)	3(5)	3(1×5)	3(1.5)	2(1×1.5)	2(5×1.5)	2(1)	1(1×1)	1	1(5×1)	3(1.5×1)	3	3	26.9	81.9
9	1(1)	3(5)	3(1×5)	3(1.5)	3(1×1.5)	3(5×1.5)	3(1.5)	2(1×1.5)	2	2(5×1.5)	1(1.5×1.5)	1	1	22.7	41.2
10	2(1.5)	1(1)	2(1×3)	3(1.5)	1(1.5×1.5)	2(1×1.5)	3(1.5)	1(1.5×1.5)	2	3(1×1.5)	1(1.5×1.5)	2	3	30.7	39.6
11	2(1.5)	1(1)	2(1×3)	3(1.5)	2(1.5×1.5)	3(1×1.5)	1(0.5)	2(1.5×0.5)	3	1(1×0.5)	2(1.5×0.5)	3	1	27.8	34.2
12	2(1.5)	1(1)	2(1×3)	3(1.5)	3(1.5×1.5)	1(1×1.5)	2(1)	3(1.5×1)	1	2(1×1)	3(1.5×1)	1	2	36.3	78.7
13	2(1.5)	2(2)	3(1×5)	1(0.5)	1(1.5×0.5)	2(3×0.5)	3(1.5)	2(1.5×1.5)	3	1(3×1.5)	3(0.5×1.5)	1	2	30.8	39.3
14	2(1.5)	2(2)	3(1×5)	1(0.5)	2(1.5×0.5)	3(3×0.5)	1(0.5)	3(1.5×0.5)	1	2(3×0.5)	1(0.5×0.5)	2	3	27.9	33.9
15	2(1.5)	2(2)	3(1×5)	1(0.5)	3(1.5×0.5)	1(3×0.5)	2(1)	1(1.5×1)	2	3(3×1)	2(0.5×1)	3	1	36.4	78.1
16	2(1.5)	3(5)	1(1×1)	2(1)	1(1.5×1)	2(5×1)	3(1.5)	3(1.5×1.5)	1	2(5×1.5)	2(1×1.5)	3	1	26.5	42.1
17	2(1.5)	3(5)	1(1×1)	2(1)	2(1.5×1)	3(5×1)	1(0.5)	1(1.5×0.5)	2	3(5×0.5)	3(1×0.5)	1	2	24	36.4
18	2(1.5)	3(5)	1(1×1)	2(1)	3(1.5×1)	1(5×1)	2(1)	2(1.5×1)	3	1(5×1)	1(1×1)	2	3	31.4	83.7
19	3(2)	1(1)	3(1×5)	2(1)	1(2×1)	3(1×1)	2(1)	1(2×1)	3	2(1×1)	1(1×1)	3	2	30.4	80.4
20	3(2)	1(1)	3(1×5)	2(1)	2(2×1)	1(1×1)	3(1.5)	2(2×1.5)	1	3(1×1.5)	2(1×1.5)	1	3	25.7	40.5
21	3(2)	1(1)	3(1×5)	2(1)	3(2×1)	2(1×1)	1(0.5)	3(2×0.5)	2	1(1×0.5)	3(1×0.5)	2	1	23.3	34.9
22	3(2)	2(2)	1(1×1)	3(1.5)	1(2×1.5)	3(3×1.5)	2(1)	2(2×1)	1	3(3×1)	3(1.5×1)	2	1	35.6	94.3
23	3(2)	2(2)	1(1×1)	3(1.5)	2(2×1.5)	1(3×1.5)	3(1.5)	3(2×1.5)	2	1(3×1.5)	1(1.5×1.5)	3	2	30.1	47.5
24	3(2)	2(2)	1(1×1)	3(1.5)	3(2×1.5)	2(3×1.5)	1(0.5)	1(2×0.5)	3	2(3×0.5)	2(1.5×0.5)	1	3	27.2	41
25	3(2)	3(5)	2(1×3)	1(0.5)	1(2×0.5)	3(5×0.5)	2(1)	3(2×1)	2	1(5×1)	2(0.5×1)	1	3	25	79.4
26	3(2)	3(5)	2(1×3)	1(0.5)	2(2×0.5)	1(5×0.5)	3(1.5)	1(2×1.5)	3	2(5×1.5)	3(0.5×1.5)	2	1	21.1	40
27	3(2)	3(5)	2(1×3)	1(0.5)	3(2×0.5)	2(5×0.5)	1(0.5)	2(2×0.5)	1	3(5×0.5)	1(0.5×0.5)	3	2	19.1	34.5

Note: A = /h, B = initial PH, C = reaction time×initial PH /h, D = aeration quantity/L·min^{-1}, E = reaction time×aeration quantity /h×L·min^{-1}, F = initial PH×aeration quantity / h×L·min^{-1}, G = amount of fillers added/g·mL^{-1}, H = reaction time×amount of fillers added/h×g·mL^{-1}, I = blank column, J = initial PH×amount of fillers added/g·mL^{-1}, K = aeration quantity×amount of fillers added/L·min^{-1}×g·mL^{-1}, L =blank column, M = blank column

Taguchi Analysis: COD removal rate versus A. reaction time B. the initial PH D. aeration quantity,...

Response Table for Means

Level	A. reaction time	B. the initial PH	D. aeration quantity	G. amount of fillers added
1	23.90	26.63	25.09	23.60
2	30.20	29.71	28.74	30.83
3	26.39	24.41	26.66	26.06
Delta	6.30	5.57	3.57	7.23
Rank	2	3	4	1

Taguchi Analysis: chroma removal rate versus A. reaction time B. the initial PH D. aeration quantity,...

Response Table for Means

Level	A. reaction time	B. the initial PH	D. aeration quantity	G. amount of fillers added
1	50.23	48.67	48.32	35.14
2	54.78	55.31	54.52	80.88
3	51.72	52.76	53.89	40.71
Delta	4.49	6.64	6.57	45.73
Rank	4	2	3	1

(a)

General Linear Model : chroma removal rate versus A. reaction time B. the initial PH D. aeration quantity G. amount of fillers added

Factor	Type	Levels	Values
A. reaction time	fixed	3	1(1) 2(1.5) 3(2)
B. the initial PH	fixed	3	1(1) 2(3) 3(5)
C. aeration quantity	fixed	3	1(0.5) 2(1) 3(1.5)
G. amount of fillers added	fixed	3	1(0.5) 2(1) 3(1.5)

Analysis of Variance for chroma removal rate, using Adjusted SS for Tests

Source	DF	Seq SS	Adj SS	Adj MS	F	P
A. reaction time	2	93.6	93.6	46.8	10.15	0.001
B. the initial PH	2	202.2	202.2	101.1	21.93	0.000
C. aeration quantity	2	216.1	216.1	108.0	23.44	0.000
G. amount of fillers added	2	11207.7	11207.7	5603.8	1215.74	0.000
Error	18	83.0	83.0	4.6		
Total	26	11802.5				

General Linear Model: COD removal rate versus A. reaction time B. the initial PH D. aeration quantity G. amount of fillers added

Factor	Type	Levels	Values
A. reaction time	fixed	3	1(1) 2(1.5) 3(2)
B. the initial PH	fixed	3	1(1) 2(3) 3(5)
C. aeration quantity	fixed	3	1(0.5) 2(1) 3(1.5)
G. amount of fillers added	fixed	3	1(0.5) 2(1) 3(1.5)

Analysis of Variance for COD removal rate, using Adjusted SS for Tests

Source	DF	Seq SS	Adj SS	Adj MS	F	P
A. reaction time	2	181.227	181.227	90.614	253.01	0.000
B. the initial PH	2	139.965	139.965	69.983	195.40	0.000
C. aeration quantity	2	57.343	57.343	28.671	80.05	0.000
G. amount of fillers added	2	243.534	243.534	121.767	339.99	0.000
Error	18	6.447	6.447	0.358		
Total	26	628.516				

(b)

Fig. 6. Results of orthogonal test analysis of internal electrolysis reaction. (a) Taguchi analysis, (b) analysis of variance, (c) interaction analysis. (*Continued*)

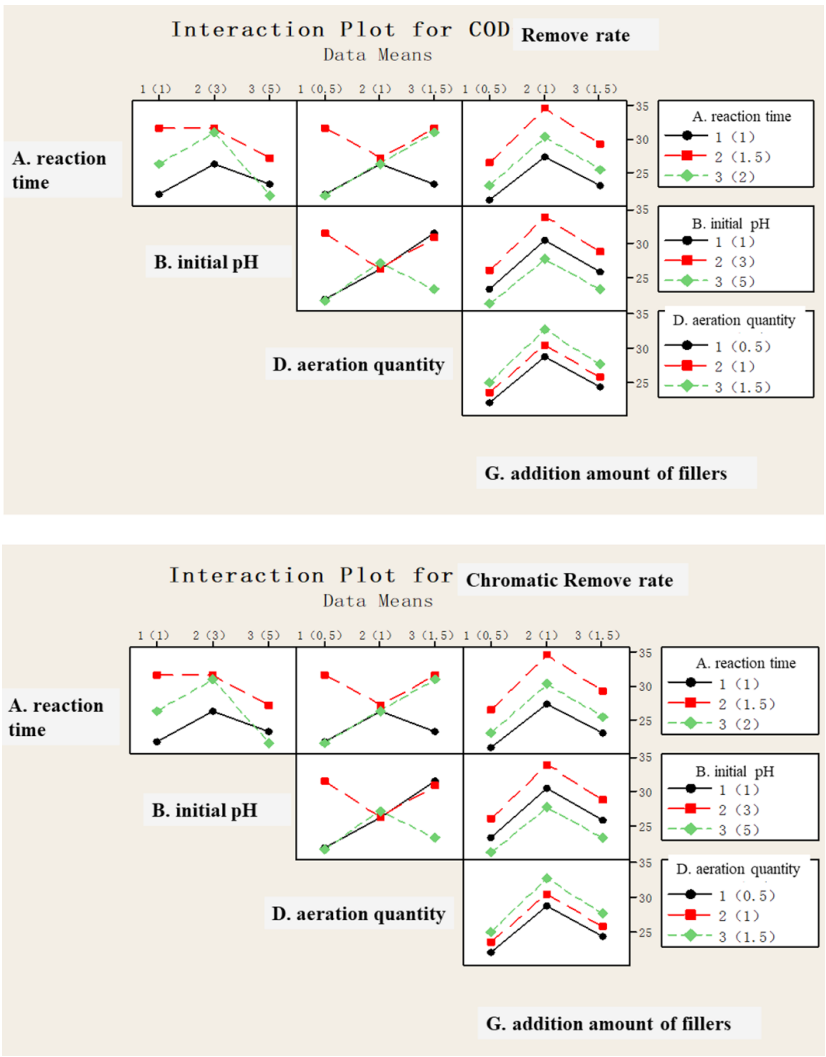

(c)

Fig. 6. (*Continued*) Results of orthogonal test analysis of internal electrolysis reaction. (a) Taguchi analysis, (b) analysis of variance, (c) interaction analysis.

Table 4
Comparison of the treatment effect of the three types of internal electrolysis packing

Packing	Iron ion/mg·L^{-1}	COD/mg·L^{-1}			Chroma /C.U.		
	Before action (after)	Inflow	After coagulation	Removal rate	Inflow	After coagulation	Removal rate
1#	57.25(53.04)	2830	1664	41.2%	268	33	87.6%
2#	52.24(49.21)	2830	1797	36.5%	268	48	82%
3#	49.07(46.45)	2830	1873	33.8%	268	59	77.9%

can reduce the aromatic ring content of lignin in raw water and degrade macromolecule high polymer organics into small molecule organics. Hence, catalytic internal electrolysis achieved the purpose of removing COD and chroma.

The groups representing the absorption peaks in the infrared spectrum of the filler surface precipitate shown in Fig. 9b are further described in Table 6 [19,20]. It is observed from Table 6 that the infrared absorption peak of the precipitate on the surface of the filler is mainly composed of iron oxides and hydroxides. At the same time, the infrared spectrum of the influent and effluent indicated that there was still a small amount of organic materials on the surface of the filler. The remaining material on the surface probably occurred because when the internal electrolysis filler was

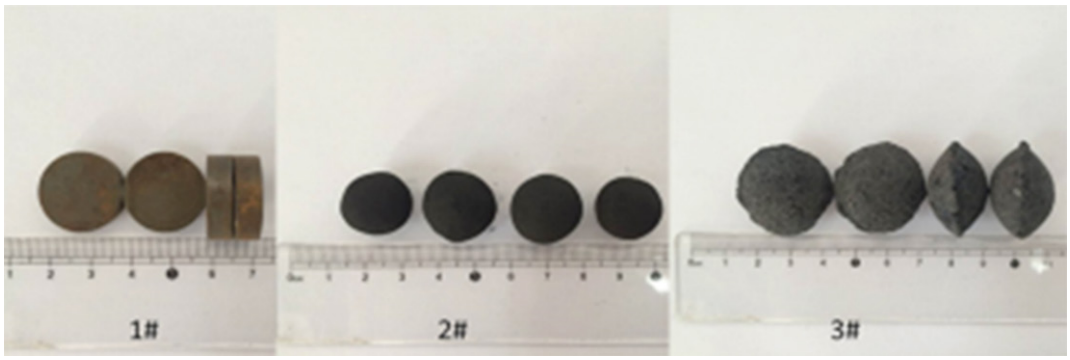

Fig. 7. The self-made internal electrolytic filler and ordinary fillers.

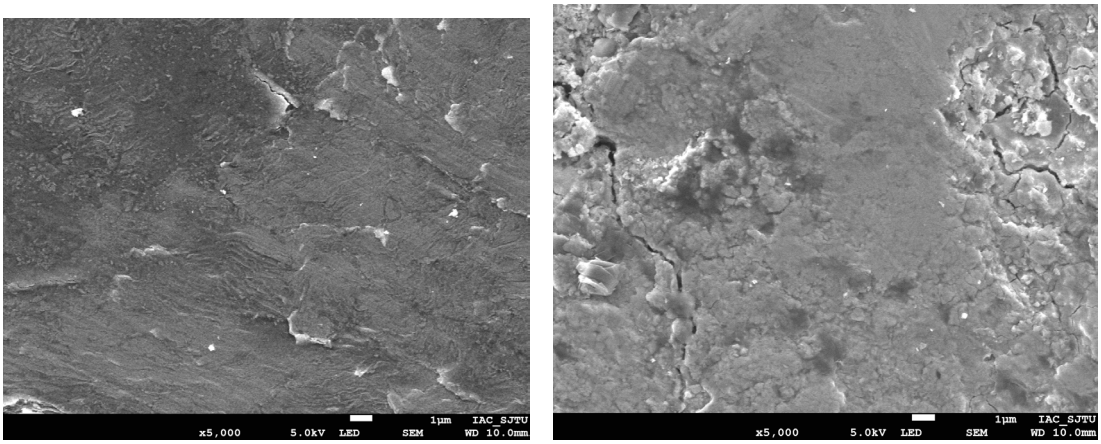

(a) Before the reaction (b) After the reaction

Fig. 8. SEM images of the iron-carbon filler before and after the reaction.

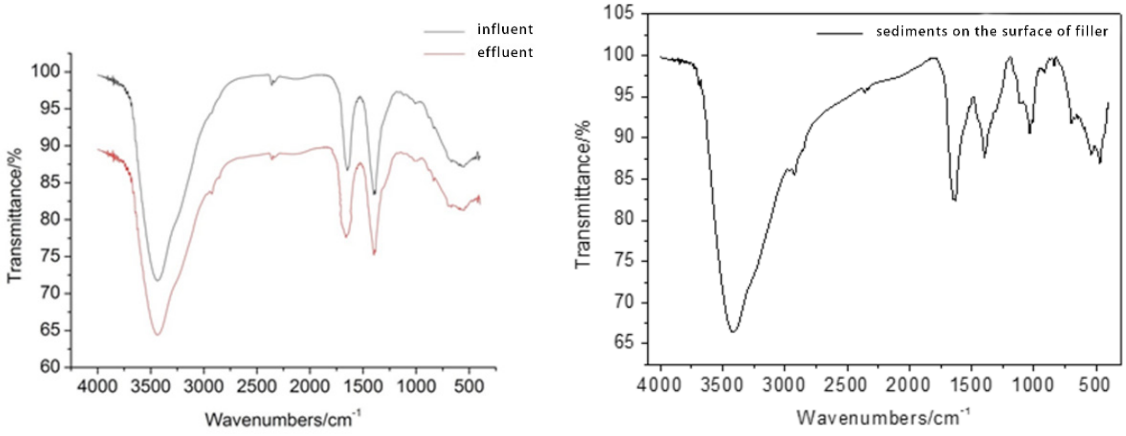

(a) influent and effluent (b) sediment on the surface of filler

Fig. 9. IR of the influent and effluent sediment on the surface of the filler.

immersed in an electrolyte solution, the filler surface formed countless micro corrosion cells, placing the surrounding solution in a micro electric field, resulting in colloid, small, suspended macromolecular organic matter and inorganic matter. The solubility of the small pollutants in the wastewater moved to the electrode surface under electrophoresis and, ultimately, formed larger flocs and adhered to the filler surface [21]. This was verified by the physical graph of the experiment. The sediment on the surface of the filler is shown in Fig 10.

Table 5
Peaks and groups in wastewater

Absorption frequency (cm^{-1})		Groups
Influent	Effluent	
3420	3420	OH telescopic vibrations of hydrogen bonding
–	2960	CH_3 bending vibration
–	2870	CH_3 bending vibration
1620	1620	Aromatic framework vibration
1453	1453	CH_2bending vibration, benzene vibration
1420	1420	Aromatic stretching vibration, C-H in-plane deformation
1172	–	C-O-C ether dissymmetry bridge stretching vibration
1110	–	Benzene C-H vibration, O-H associated light band
1059	–	Benzene C-H vibration, C=Ostretching vibration

Table 6
Peaks and groups of sediment on the surface of the filler

Absorption frequency (cm^{-1})	Groups
3420	Hydrogen association of OHstretching vibration
2960	CH_3 bending vibration
1620	Aromatic framework vibration
1380	Benzene stretching vibration, C-H in-plane deformation
1040	Benzene stretching vibration, C-H in-plane deformation
880	Fe-OH-Febending vibration
580	Fe-O vibration

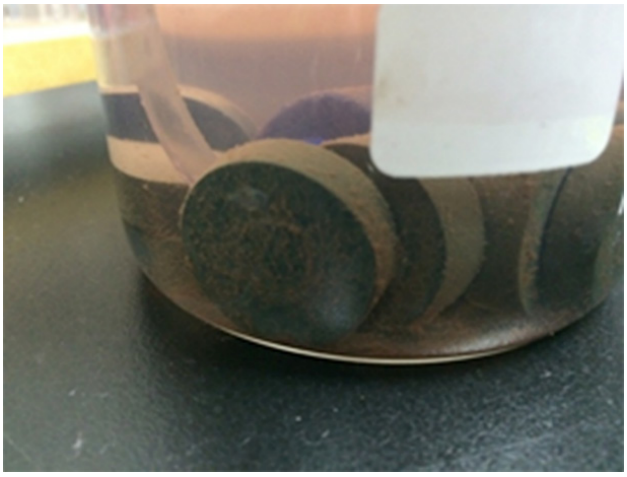

Fig. 10. Sediment on the surface of the filler.

7. Conclusion

In summary, the optimum conditions for catalytic internal electrolysis are an initial pH 3.0, reaction time of 1.5 h, aeration quantity of 1.0 L/min and amount of added fillers of 1 g/mL, as determined by a single factor experiment and an orthogonal experimental design. The results showed that under the optimum conditions, the self-made ultrafine grinding catalytic internal electrolytic filler had a better performance than standard fillers and that 37.0% and 88.4% removal rates of COD and chroma were achieved, respectively. According to orthogonal experimental variance analysis, the effects of the initial pH, reaction time, aeration quantity and amount of added fillers on the treatment are extremely significant. The impact they had on COD removal was: amount of added fillers > reaction time > initial pH > aeration quantity. The impact they had on chroma removal was: amount of added fillers > aeration quantity> initial pH > reaction time. Moreover, the four factors had a significant interaction.

The IR spectra of pulping wastewater before and after treatment showed that catalytic internal electrolysis reduced the aromatic ring content of lignin in raw water and degraded macromolecular high polymer organic matter into small molecule organic matter, which improved the biodegradability of wastewater. IR spectral analysis of the surface precipitates of the filler demonstrated that the main components were iron oxides and hydroxides and contained a small amount of organic matter, which indicated that the organic matter in the wastewater moved to the surface of the electrode under the action of a micro-electric field and then eventually formed a larger floc on the surface of the filler. This phenomenon indicates that internal electrolysis has the effect of electricity collection.

Acknowledgement

The authors would like to acknowledge the financial support from the China Central University scientific research basic business fee items(Grant No.: 2015WK01)

References

[1] L. Shuhui, Y. Qiujuan, Papermaking industry clean production, environmental protection, recycling, Beijing, Chemical Industry Press, 2007.
[2] S. Park, S. Lee, J. Han, Effect of coagulation pretreatment on microfiltration of paper mill wastewater using electrospun membranes, Desal. Water Treat., 77 (2017) 83–88.

[3] C.M. Sheridan, K.G. Harding, A. Brink, The Fenton oxidation of biologically treated paper and pulp mill effluents: A performance and kinetic study, Process Safety Environ. Protect., 107 (2017) 206–215.
[4] K. Sudarshan, P. Kotteeswaran, Reuse the pulp and paper industry wastewater by using fashionable technology, Appl. Water Sci., 7(6) (2017) 3317–3322.
[5] B.R. Yadav, A. Garg, Hetero-catalytic hydrothermal oxidation of simulated pulping effluent: Effect of operating parameters and catalyst stability, Chemosphere, 191 (2017) 128–135.
[6] X.J. Zhou, N.Q. Ren, W.Q. Guo, A review on treatment methods of dye wastewater, CIESC J., 101 (2013) 23983–23992.
[7] J.X. Lv, Y. Cui, Treatment of reactive red X-3B dye wastewater with Cu-Fe inner electrolysis method, China Dyeing Finish., 7 (2015) 17–20.
[8] K. Yin, P.H. Rao, I. Lo, M.S.H. Mak, H.R. Dong, Lab-scale simulation of the fate and transport of nano zero-valent iron in subsurface environments: Aggregation, sedimentation and contaminant desorption, J. Hazard. Mater., 228 (2012) 118–125.
[9] X.B. Zhang, W. Yang, F.Y. Sun, W.Y. Dong, J. Dong, Degradation efficiency and mechanism of azo dye RR2 by a novel ozone aerated internal micro-electrolysis filter, J. Hazard. Mater., 276 (2014) 77–87.
[10] Z.P. Xu, G.Y. Song, J.H. Luo, G.R. Qing, J.Y. Liu, Mechanism of enhanced nitrate reduction via micro-electrolysis at the powdered zero-valent iron/activated carbon interface, J. Colloid Interf. Sci., 435 (2014) 21–25.
[11] J.J. Yang, X.J. Xu, G. Wang, R. Nie, X. Li, K.Y. Gao, Treatment of wastewater containing copper by coupling electrolysis with intensified micro-electrolysis, Chinese J. Nonferr. Metal, 23(10) (2013) 2936–2941.
[12] J. Wu, L.T. Pan, Y. Han, Advanced treatment of biologically pretreated coking wastewater by intensified zero-valent iron process (IZVI) combined with anaerobic filter and biological aerated filter (AF/BAF), J. Central South Univ., 22(10) (2015) 3781–3787.
[13] L.T. Pan, Y. Han, A novel anoxic-aerobic biofilter process using new composite packing material for the treatment of rural domestic wastewater, Water Sci. Technol., 73(10) (2016) 2486–2492.
[14] C.Y. Zhang, Research of Advanced Treatment of Livestock Wastewater by Subsurface Flow Constructed Wetland. Master's thesis. Zhengzhou University, 2012.
[15] L.M. Ma, Y.Y. Gu, K. Feng, Research on optimum coagulation conditions and pH variation of acidic chemical wastewater pretreated by catalyzed iron and coagulation process, Water Resour. Water Eng., 24(3) (2013) 50–53.
[16] L. Zhiyuan, Study on Fenton Oxidation-Coagulation Method of Biologically Treated Coal-chemical Engineering Wastewater. Master's thesis. Harbin Institute of Technology, 2013.
[17] A.S. Lea, D.J. Gaspar, M.H. Engelhard, D.R. Baer. R.M, P.G. Tratnyek, Evidence for localization of reaction upon reduction of carbon tetrachloride by granular iron, Langmuir, 18(20) (2002) 7688–7693.
[18] O. Faix, Classification of lignins from different botanical origins by FT-IR spectroscopy, Holzforschung, 45S (1991) 21–27.
[19] S. Hanchang, C. Can, Study on the iron chip surface chemistry of iron chip process treating wastewater containing dyes, Environ. Chem., 23(1) (2004) 90–95.
[20] T.L. Johnson, W. Fish, P.G. Tratnyek, Y.A. Gorby, Degradation of carbon tetrachloride by iron metal: Complexation effects on the oxide surface, J. Contam. Hydrology, 29(4) (1998) 379–398.
[21] X. Xiao, Treating pulping middle stage effluent by microelectrolysis method, Sci. Technol., 24(6) (2005) 102–105.